

**OPTIMISATION OF SINGLE SLOPE SOLAR
STILL TO DESALINATE SEAWATER FOR
HYDROGEN HARVESTING APPLICATION**



ONG CHEAH MENG

UMS
UNIVERSITI MALAYSIA SABAH

**FACULTY OF ENGINEERING
UNIVERSITI MALAYSIA SABAH**

2016

CERTIFICATION

NAME : **ONG CHEAH MENG**

MATRIX NO. : **PK20118240**

TITLE : **OPTIMISATION OF SINGLE SLOPE SOLAR STILL TO
DESALINATE SEAWATER FOR HYDROGEN HARVESTING
APPLICATION**

DEGREE : **MASTER OF ENGINEERING
(MECHANICAL)**

VIVA DATE : **07 DECEMBER 2015**



APPROVED BY
UMS
UNIVERSITI MALAYSIA SABAH

1. SUPERVISOR

Prof. Dr. Yeo Kiam Beng @ Abdul Noor

Signature

DECLARATION

I hereby declare that the material in this thesis is my own except for the quotations, excerpts, equations, summaries and references, which have been duly acknowledged.

10 July 2015

.....

Ong Cheah Meng

PK20118240



UMMS
UNIVERSITI MALAYSIA SABAH

ACKNOWLEDGEMENT

I would like to express my deepest gratitude and appreciation to my supervisor, Prof. Dr. Yeo Kiam Beng @ Abdul Noor, for his guidance and teaching to complete this thesis, in particular for his wisdom and his knowledge in the field of Heat Transfer Analysis and Modeling. It has been a special experience for me to be supervised under him. And also not forgetting my co-supervisor, Mr. Kenneth Teo Tze Kin, for all his advices, guidance and support in this research work.

Furthermore, I would also wish to thank Mr. Yoong Hou Pin and Mr. Choong Wai Heng for their technical support in this research work. Not to forget also the supports from the Faculty of Engineering (FKJ), Universiti Malaysia Sabah (UMS) and the Materials and Minerals Research Unit (MMRU), Faculty of Engineering (FKJ), Universiti Malaysia Sabah (UMS) for providing the facilities, tools, equipment, and financial support necessary to complete this research work.

Throughout this period, the constant love, support, encouragement and confidence given to me by my parents, Mr. and Mrs. Ong are the reasons I am able to stand up for the challenges in pursuing my Higher Education. I am also fortunate to have a best friend like Mr. Wong Wei Loong who is always available to help me overcome various obstacles through his unflinching support and advice.

Ong Cheah Meng

PK20118240

ABSTRACT

The challenging efforts of this project have been designed to explore the abundance of renewable solar energy for the desalination of the inexhaustible seawater resource for the production of the most critical clean water resource necessary for the human consumption and existence, in particular to the poorer rural populations. The working principle of a solar still has been based on the heat transfer processes of three major components of the solar still (glass cover, seawater and basin) and its surrounding as a result of exposing the system to the solar irradiance. Two analytical approaches have been utilized to develop the theoretical model and the numerical model by forward finite difference approach for predicting the solar still performance. However, the numerical model has shown to be significantly far more accurate in predicting the experimental results than the theoretical model, particularly in a less consistent and varied solar irradiance during the latter part of the afternoon hours. At the same time, the optimization of the single slope solar still as a simple, effective, safe and user friendly water treatment device, for the production of clean water has been experimentally verified. The experimental result has found that the optimum slope angle required is six degree (6°), and the optimum volume amount of seawater is three litres (3 L) for the solar still to produce the optimum clean water production at 1.4 litres per sunny day. A simulation feasibility study consists of the optimized single slope solar still with a PEM electrolyzer of an output rating of 2.5 litres/minute has also been conducted to achieve a yield production of 1,335 litres of hydrogen gas under the atmospheric pressure, which has an equivalence of about 4.7kWh of electricity.

ABSTRAK

PENGOPTIMUMAN 'SOLAR STILL' CERUN TUNGGAL UNTUK PENGUAPAN AIR LAUT BAGI APLIKASI PENUAIAN HIDROGEN

Semua usaha cabaran dalam projek ini telah direka untuk menerokai penggunaan tenaga solar yang banyak untuk tujuan penguapan sumber air laut yang tidak habis-habis bagi proses penghasilan sumber air bersih yang amat kritikal untuk menanggung keperluan harian manusia, terutama di kawasan populasi luar bandar yang miskin. Prinsip utama 'Solar Still' adalah berdasarkan proses-proses pemindahan haba antara tiga komponen utama dalamnya (penutup kaca, air laut dan besin) dengan persekitarannya semasa didedahkan bawah sinaran solar. Dua cara analisis telah digunakan untuk mendapatkan model teori dan model berangka dengan cara 'forward finite difference' untuk meramalkan prestasi 'Solar Still'. Akan tetapi, model berangka didapati boleh meramal keputusan eksperimen dengan lebih tepat berbanding dengan model teori, terutamanya pada waktu petang dimana sinaran solar adalah berubah dan tidak konsisten. Pada waktu yang sama, pengoptimuman 'Solar Still' cerun tunggal sebagai alat rawatan air yang mudah, berkesan, selamat dan mesra pengguna untuk penghasilan air bersih telah disahkan secara eksperimen. Keputusan eksperimen mendapati bahawa sudut enam darjah adalah sudut optimum (6°), dan tiga liter adalah isipadu optimum air laut bagi 'Solar Still' untuk penghasilan air bersih 1.4 liter pada setiap hari siang. Simulasi kajian kebolehlaksanaan yang terdiri daripada 'Solar Still' cerun tunggal yang telah dioptimalkan dengan satu alat elektrolisis PEM dengan kuasa penghasilan sebanyak 2.5 liter setiap minit telah dilaksanakan dan keputusan simulasi menunjukkan penghasilan sebanyak 1,335 liter gas hydrogen bawah tekanan atmosfera, juga bersamaan dengan penjanaan kuasa elektrik sebanyak 4.7 kWh.

TABLE OF CONTENTS

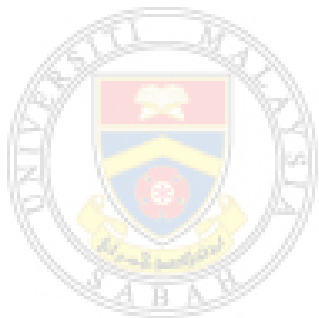
	Page
TITLE	i
DECLARATION	ii
ACKNOWLEDGEMENT	iii
ABSTRACT	iv
<i>ABSTRAK</i>	v
LIST OF CONTENTS	vi
LIST OF TABLES	xi
LIST OF FIGURES	xiii
LIST OF ABBREVIATIONS	xx
LIST OF SYMBOLS	xxi
CHAPTER 1: INTRODUCTION	1
1.1 Overview	1
1.2 Single Slope Solar Still	2
1.3 Seawater Desalination	3
1.4 Hydrogen Harvesting	4
1.5 Challenges	5
1.6 Objective	7
1.7 Scope of Work	7
1.8 Thesis Organization	8

CHAPTER 2: LITERATURE REVIEW	10
2.1 Overview	10
2.2 Classification of Water	10
2.3 Seawater Desalination Technology	11
2.4 Solar Still for Seawater Desalination	13
2.4.1 Solar Still with Modifications	16
2.4.2 Heat and Mass Transfer Model	17
2.4.3 Solar Still Optimum Operating Conditions	20
2.4.4 Passive Solar Still Efficiency	22
2.5 Hydrogen Harvesting	23
2.5.1 Water Electrolysis	24
2.5.2 Conventional Hydrogen Storage	25
2.5.3 Simulation of Hydrogen Gas Production	26
2.6 Summary of Literature Review	28
CHAPTER 3: THEORETICAL MODELLING	30
3.1 Overview	30
3.2 Heat Transfer Processes in the Single Slope Solar Still	30
3.2.1 Radiation Heat Transfer Process	31
3.2.2 Convection Heat Transfer Process	33
3.2.3 Conduction Heat Transfer Process	33
3.3 Single Slope Solar Still Heat Transfer Model	34
3.3.1 Glass Cover Heat Transfer Coefficients	37
3.3.2 Basin Heat Transfer Coefficients	38
3.3.3 Seawater Heat Transfer Coefficients	38
3.3.4 Heat Transfer Temperature Governing Equation	39
3.3.5 Solving Heat Transfer Temperature Governing Equation	42
3.3.6 Critical Clean Water Mass and Solar Still Efficiency	43
3.3.7 Simulation Result	44
3.4 Temperature Distribution of the Single Slope Solar Still by Finite Difference Method	49

3.4.1	Governing Equations for Nodes on the Glass Cover	53
3.4.2	Governing Equations for Interior Nodes	56
3.4.3	Governing Equations for Nodes on the Solar Still Walls	57
3.4.4	Simulation Results	61
3.5	Summary	65
CHAPTER 4: EXPERIMENT		67
4.1	Overview	67
4.2	Single Slope Solar Still Prototype Design and Fabrication	67
4.3	Experimental Preparations	71
4.3.1	Experimental Objectives	71
4.3.2	Experimental Location	72
4.3.3	Apparatus	73
4.3.4	Experimental Setup and Procedure	75
4.3.5	Safety Precautions	78
4.4	Clean Water Quality Laboratory Test	79
4.4.1	Atomic Absorption Spectroscopy (AAS) Test Introduction	80
4.4.2	Atomic Absorption Spectroscopy (AAS) Test Preparation	81
4.4.3	AAS Machine Calibration Process	83
4.5	Summary	86
CHAPTER 5: OPTIMIZATION OF SINGLE SLOPE SOLAR STILL		87
5.1	Overview	87
5.2	Climate Condition of Experimental Location	87
5.2.1	Trend of Sunny Days	88
5.2.2	Average Solar Irradiance Trend	89
5.2.3	Average Wind Speed and Wind Direction Trend	91
5.2.4	Average Ambient Temperature Trend	92
5.3	Optimum Solar Still Performance for Different Slope Angles	94
5.3.1	Average Glass Cover Temperature for Different Slope Angle	94
5.3.2	Average Seawater Temperature for Different Slope Angles	96

5.3.3	Average Basin Temperature for Different Slope Angles	97
5.3.4	Clean Water Productivity for Different Slope Angles	98
5.4	Optimum Solar Still Performance for Different Seawater Volumes	100
5.4.1	Average Glass Cover Temperature for Different Seawater Volumes	100
5.4.2	Average Seawater Temperature for Different Seawater Volumes	101
5.4.3	Average Basin Temperature for Different Seawater Volumes	102
5.4.4	Clean Water Production for Different Seawater Volumes	104
5.5	Average Temperature Distribution of Optimized Single Slope Solar Still	106
5.5.1	Average Basin Temperature Distribution (Top View)	106
5.5.2	Average Glass Cover Temperature Distribution (Top View)	109
5.5.3	Average Solar Still Temperature Distribution (Side View)	112
5.6	Summary	115
CHAPTER 6: SIMULATION OF HYDROGEN PRODUCTION		116
6.1	Overview	116
6.2	Integrated System Introduction	116
6.3	Integrated System Simulation Model	117
6.4	Simulation Result and System Feasibility	121
6.5	Summary	126
CHAPTER 7: RESULT AND DISCUSSION		127
7.1	Overview	127
7.2	Optimized Solar Still Performance	127
7.2.1	Governing Response of Solar Irradiance and Ambient Temperature	128
7.2.2	Optimized Average Glass Cover Temperature	130
7.2.3	Optimized Average Seawater Temperature	132
7.2.4	Optimized Average Basin Temperature	133
7.2.5	Optimized Average Accumulated Clean Water Mass	135
7.2.6	Instantaneous Efficiency	136

7.3	Clean Water Quality Test Result	137
	7.3.1 AAS Test Results	137
7.4	Summary	140
CHAPTER 8: CONCLUSION		141
8.1	Overview	141
8.2	Conclusion	142
8.3	Future Work	144
REFERENCES		xxiv

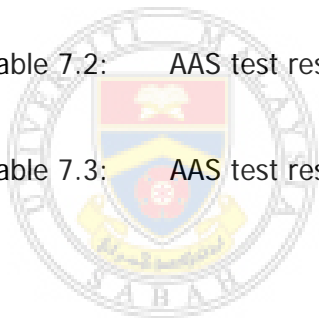


UMS
UNIVERSITI MALAYSIA SABAH

LIST OF TABLES

	Page
Table 2.1: Categorization of seawater desalination processes	12
Table 2.2: Efficiencies of different solar still design	22
Table 3.1: Solar Still operating parameters defined for simulation purpose	44
Table 3.2: Simulation parameters for the temperature distribution model	62
Table 4.1: Single Slope Solar still slope angles corresponding to its respective latitude coordinate of experimental location	68
Table 4.2: Requirements for distilled water	80
Table 4.3: Calcium element calibration result	84
Table 4.4: Magnesium element calibration result	85
Table 4.5: Sodium concentration calibration result	86
Table 5.1: Average glass cover temperature for different slope angles	95
Table 5.2: Average seawater temperature recorded for different slope angles	96
Table 5.3: Average basin temperature recorded for different slope angles	97
Table 5.4: Average mass of clean water collected for different slope angles	99

Table 5.5:	Average glass cover temperature recorded for different seawater volumes	100
Table 5.6:	Average seawater temperature for different seawater volumes	102
Table 5.7:	Average basin temperature recorded for different water volumes	103
Table 5.8:	Average mass of clean water collected for different seawater volumes	104
Table 6.1:	Parameters defined in the Simulink model	121
Table 7.1:	AAS test result for the Calcium element	138
Table 7.2:	AAS test result for the Magnesium element	139
Table 7.3:	AAS test result for the Sodium element	139



LIST OF FIGURES

	Page
Figure 2.1: Water salinity scale for different types of water in parts per thousand (ppt).	11
Figure 2.2: Total Dissolved Solids (TDS) chart for different freshwater sources in parts per million (ppm).	11
Figure 2.3: Passive single slope solar still.	14
Figure 2.4: Active single slope solar still.	14
Figure 2.5: Inverted solar still.	15
Figure 2.6: Vertical solar still.	15
Figure 2.7: Schematic diagram of the tilted wick type solar still.	16
Figure 2.8: Comparison of the Hongfei <i>et al.</i> (2002) model with the Dunkle (1961) model.	18
Figure 2.9: Comparison study of different mathematical models with respective correlation coefficient and percentage deviation.	19
Figure 2.10: Effect of the wind speed on the daily output of a solar still under a typical summer day in Jeddah.	21
Figure 2.11: Proton Exchange Membrane electrolyzer operational diagram.	25
Figure 2.12: Effect of the cooling temperature to the absorption rate of the metal hydride.	26
Figure 3.1: Conceptual illustration of heat transfer process.	31

Figure 3.2:	Spectrum of sunlight radiation.	32
Figure 3.3:	Various heat transfer quantities in the single slope solar still	36
Figure 3.4:	The average solar irradiance regression model versus time in Kota Kinabalu, Sabah, for a period of January 2013 to December 2014.	45
Figure 3.5:	The simulated accumulated mass of clean water produced against time.	45
Figure 3.6:	The simulated glass cover temperature and seawater temperature versus time.	46
Figure 3.7:	Effect of different volume of seawater in the basin to the productivity of the solar still.	47
Figure 3.8:	Effect of different wind speed to the productivity of the solar still during the first one hundred minutes.	48
Figure 3.9:	Effect of different wind speed to the productivity of the solar still during the last one hundred minutes.	48
Figure 3.10:	Grid system of single slope solar still showing side-view nodes.	51
Figure 3.11:	Illustration of the cross sectional side view of the solar still.	51
Figure 3.12:	Example of an interior node and its neighbour nodes.	52
Figure 3.13:	Illustration of node-1 location and its surrounding nodes.	53
Figure 3.14:	Illustration of node locations between node-1 and node-16 and its respective surrounding nodes.	54

Figure 3.15:	Illustration of the node-16 and its surrounding nodes.	55
Figure 3.16:	Illustration of interior node locations and its respective surrounding nodes.	56
Figure 3.17:	Illustration of node locations along the sides of the solar still and its respective surrounding nodes.	58
Figure 3.18:	Illustration of node-28 location and its surrounding nodes.	59
Figure 3.19:	Illustration of node-33 location and its surrounding nodes.	59
Figure 3.20:	Illustration of node-29, node-30, node-31 and node-32 locations and its respective surrounding nodes.	60
Figure 3.21:	The simulated temperature distribution of single slope solar still from 8:00 a.m. until 9:00 a.m.	63
Figure 3.22:	The simulated temperature distribution of single slope solar still from 10:00 a.m. until 1:00 p.m.	63
Figure 3.23:	The simulated temperature distribution of single slope solar still from 2:00 p.m. until 3:00 p.m.	64
Figure 3.24:	The simulated temperature distribution of single slope solar still from 4:00 p.m. until 6:00 p.m.	64
Figure 4.1:	The side view details of the solar still prototype for a six degree slope angle (dimension in mm).	69
Figure 4.2:	The front view details of the solar still prototype for six degree slope angle (dimension in mm).	69

Figure 4.3:	The isometric view of the solar still prototype for a six degree slope angle.	70
Figure 4.4:	Fabricated single slope solar still prototype with insulation and water hoses installed.	71
Figure 4.5:	Satellite map of the experimental location selected.	73
Figure 4.6:	Snapshot of the experimental location selected.	73
Figure 4.7:	The Graphtec Midi logger GL820 data logger.	74
Figure 4.8:	The Solar Predictor™ weather data logger.	75
Figure 4.9:	The arrangement of the five solar stills during the experiment.	76
Figure 4.10:	The Graphtec data logger encased in plastics box with heat sink.	77
Figure 4.11:	Extension power socket for the data logger.	77
Figure 4.12:	The weather data logger setup during the experiment.	78
Figure 4.13:	The Flame type Perkin Elmer 4100 Atomic Absorption Spectrometry Machine.	82
Figure 4.14:	The laboratory pH meter.	83
Figure 4.15:	Calcium element calibration result.	84
Figure 4.16:	Magnesium element calibration result.	85
Figure 4.17:	Sodium element calibration comparison plot.	86

Figure 5.1:	Number of sunny days at the experimental location in year 2013 and 2014.	88
Figure 5.2:	Average maximum solar irradiance (W/m^2) of sunny days recorded for the months between the years 2013 and 2014.	89
Figure 5.3:	Average solar irradiance values at different hours during sunny days at Kota Kinabalu, Sabah, Malaysia.	90
Figure 5.4:	Average maximum wind speed recorded in year 2013 and 2014.	91
Figure 5.5:	Average wind direction radar plot for year 2013 and year 2014.	92
Figure 5.6:	Average ambient temperature recorded in year 2013 and 2014.	93
Figure 5.7:	Average ambient temperature recorded in a day in year 2013 and 2014.	94
Figure 5.8:	Average glass cover temperature against time for different slope angles.	95
Figure 5.9:	Average seawater temperature recorded against time for different slope angles.	96
Figure 5.10:	Average basin temperature recorded against time for different slope angles.	98
Figure 5.11:	Average accumulated mass of clean water collected against time for different slope angles.	99
Figure 5.12:	Average glass cover temperature recorded against time plot for different seawater volumes.	101

Figure 5.13:	Average seawater temperature recorded against time for different seawater volumes.	102
Figure 5.14:	Average basin temperature recorded against time for different seawater volumes.	103
Figure 5.15:	Average accumulated mass of clean water collected against time for different seawater volumes.	105
Figure 5.16:	Curve fitting trends of the accumulated mass of clean water produced versus solar still slope angles for different seawater volumes.	105
Figure 5.17:	Colour-map temperature distribution plots for the average basin temperature (top view) from 8 a.m. until 1 p.m.	107
Figure 5.18:	Colour-map temperature distribution plots for the average basin temperature (top view) from 2 p.m. until 6 p.m.	108
Figure 5.19:	Colour-map temperature distribution plots for the average glass cover temperature (top view) from 8 a.m. until 1 p.m.	110
Figure 5.20:	Colour-map temperature distribution plots for the average glass cover temperature (top view) from 2 p.m. until 6 p.m.	111
Figure 5.21:	Colour-map temperature distribution plots for the middle sectional side view from 8 a.m. until 1 p.m.	113
Figure 5.22:	Colour-map temperature distribution plots for the middle sectional side view from 2 p.m. until 6 p.m.	114
Figure 6.1:	Single slope solar still integrated hydrogen harvesting system flow diagram.	117
Figure 6.2:	Complete Simulink model for the proposed integrated system.	118

Figure 6.3:	Single slope solar still sub-system Simulink model.	120
Figure 6.4:	PEM electrolyzer Simulink model.	121
Figure 6.5:	Simulated basin and glass cover temperature versus time.	122
Figure 6.6:	Simulated accumulative mass of clean water versus time.	123
Figure 6.7:	Volume of hydrogen gas produced versus time for different PEM electrolyzer output rates.	124
Figure 6.8:	Mass of clean water left versus time for different PEM electrolyzer output rates.	125
Figure 7.1:	4 th order polynomial best fitted curve of average solar irradiance.	128
Figure 7.2:	4 th order polynomial best curve fitted of ambient temperature.	130
Figure 7.3:	Daily average glass cover temperature distribution comparison.	131
Figure 7.4:	Average seawater daily temperature distribution comparison.	133
Figure 7.5:	Average basin daily temperature distribution comparison.	134
Figure 7.6:	Average accumulated mass of clean water comparison.	135
Figure 7.7:	Instantaneous efficiency comparison plot.	137

LIST OF ABBREVIATIONS

AAS	-	Atomic Absorption Spectroscopy
AEC	-	Alkaline Electrolysis Cells
CFD	-	Computational Fluid Dynamics
ED	-	Electrodialysis
EDL	-	Electrodeless discharge lamp
GPS	-	Global Positioning System
HCL	-	Hollow cathode lamp
MED	-	Multiple-effect distillation
MSF	-	Multi-stage flash
PCM	-	Phase Change Materials
PEM	-	Proton Exchange Membrane
ppm	-	parts per million
ppt	-	parts per thousand
PTFE	-	Polytetrafluoroethylene
RO	-	Reverse Osmosis
SOEC	-	Solid Oxide Electrolysis Cells
TDS	-	Total Dissolved Solids
VC	-	Vapour Compression

LIST OF SYMBOLS

A	-	Surface area (m ²)
a	-	Absorptivity
C_{paf}	-	Specific heat capacity of humid air at an average temperature (J/kg.°C)
C_p	-	Specific heat (J/kg.°C)
E_{gen}	-	Internal rate of heat generated (Watt)
$\Delta E_{m,n}$	-	Change of energy content of the node (Joule)
G	-	Solar irradiance (W/m ²)
h	-	Heat transfer coefficient (W/m ² .°C)
h_{fg}	-	Latent heat of evaporation (kJ/kg.°C)
k	-	Thermal conductivity (W/m.°C)
L	-	Distance (m)
L_e	-	Lewis number
M_w	-	Molecular weight of water vapour (kg/mol)
$(MC)_w$	-	Seawater heat capacity rate per unit area (J/m ² .°C)
m	-	Mass (kg)
\dot{m}_{evp}	-	Mass flow rate of the evaporated seawater (kg/s)
P	-	Pressure (Pa)
ρ	-	Density (kg/m ³)
Q	-	Rate of heat transfer (Watt)
q	-	Heat flux (W/m ²)

$R(x)$	-	Truncation error
T	-	Temperature ($^{\circ}\text{C}$)
Δt	-	Time step (s)
V	-	Wind speed (m/s)
v	-	Volume (ml)
Δx	-	Distance between two nodes along the x-axis (m)
Δy	-	Distance between two nodes along the y-axis (m)
σ	-	Stefan-Boltzmann constant ($5.64 \times 10^{-8} \text{ W/m}^2 \cdot ^{\circ}\text{C}^4$)
θ	-	Slope angle (rad)
ε_g	-	Glass cover emissivity
η	-	Instantaneous efficiency (%)



UMS
UNIVERSITI MALAYSIA SABAH